JOURNAL OF APPLIED ELECTROCHEMISTRY 21 (1991) 575–582

Electrochemical and XPS studies of the surface oxidation of synthetic heazlewoodite (Ni_3S_2)

A. N. BUCKLEY

CSIRO Division of Coal and Energy Technology, PO Box 136, North Ryde, NSW 2113, Australia

R. WOODS

CSIRO Division of Mineral Products, PO Box 124, Port Melbourne, Victoria 3207, Australia

Received 9 November 1990; revised 16 January 1991

X-ray photoelectron spectroscopic (XPS) and electrochemical techniques have been applied to the investigation of the surface oxidation of synthetic heazlewoodite (Ni_3S_2). The XPS data showed that exposure of the sulphide to air resulted in nickel atoms migrating to the surface to form an overlayer of a hydrated nickel oxide and leave a sulphur-rich heazlewoodite. A hydrated nickel oxide was also produced on immersion of heazlewoodite in acetic acid solution in equilibrium with air, despite nickel being soluble under these conditions. After the acetic acid treatment, the S(2p) spectrum had a component at the binding energy of NiS and a small contribution due to sulphur-oxygen species. Voltammetry with bulk heazlewoodite electrodes, and the ground sulphide in a carbon paste electrode, indicated that, at pH 4.6, the initial anodic product was a sulphur-rich heazlewoodite and that oxidation was inhibited when NiS was formed on the surface. Further oxidation to higher nickel sulphides and elemental sulphur occurred at high potentials. In basic solutions, oxidation was restricted due to the formation of nickel oxide.

1. Introduction

Nickel forms a series of sulphides of which heazlewoodite (Ni_3S_2) is the most nickel-rich member [1]. The other stable phases at ambient temperatures are godlevskite (Ni_7S_6), millerite (NiS), polydymite (Ni_3S_4) and vaesite (NiS_2).

Electrochemical investigations have been carried out [2–6] to elucidate the leaching characteristics of nickel sulphides that are important in the winning of nickel from its ores. Kato and Oki [2, 3] studied the anodic oxidation of heazlewoodite and millerite in acid solutions using voltammetric and galvanostatic techniques. The results were explained in terms of the oxidation of Ni_3S_2 to NiS which could be oxidized further to elemental sulphur or sulphate. Power [4, 5] applied rotating ring disc electrodes to study the anodic oxidation of these sulphides in acid solutions. The formation of a sulphur-rich sulphide layer was found to passivate the surface of both minerals with a transpassive region in which sulphur oxyanions were formed. Price and Davenport [6] investigated the anodic reactions of Ni_3S_2, NiS and nickel under galvanostatic conditions. These authors interpreted potential steps on the charging curves in terms of oxidation through the series of phases: Ni_3S_2–$Ni_{1.5}S_2$–$Ni_{1.2}S_2$–NiS_2–S^0. X-ray diffraction (XRD) analysis of reaction residues revealed only heazlewoodite, millerite and elemental sulphur structures, but it was considered that changes in composition of the products could have occurred between the end of anodic treatment and the XRD analysis.

Marcus *et al.* [7] determined the photoelectron spectra of Ni_3S_2 prepared by sulphidizing nickel metal as part of a study of the influence of sulphur on the passivation of nickel. The observed $Ni(2p)_{3/2}$ binding energy for Ni_3S_2 was found to be close to that of nickel metal (852.8 eV); a binding energy similar to that for the corresponding metal is typical of metal sulphides. However, the $S(2p)_{3/2}$ binding energy of 162.2 eV was higher than for similar sulphides. Values for galena (PbS), sphalerite (ZnS), chalcocite (Cu_2S), chalcopyrite ($CuFeS_2$), bornite (Cu_5FeS_4), and pyrrhotite ($Fe_{1-x}S$) are all no greater than 161.6 eV [8–12]. The value for heazlewoodite is close to that of pyrite (162.4 eV) [13] in which the sulphur atoms are paired as S_2 units with a formal valence state of −II. Some binding energy values reported in the literature for sulphides are unreliable since the specimens were exposed to air before examination. However, the Ni_3S_2 examined by Marcus *et al.* [7] had been prepared, and spectra recorded, without the sample being removed from the vacuum and was free from oxidation products.

Values for the S(2p) binding energy of NiS have been reported to be similar to that of Ni_3S_2 [for example: 14, 15], but Grzetic [16] reported a $S(2p)_{3/2}$ binding energy of 161.3 eV. The S(2p) binding energy of NiS_2 has been reported as 162.7 eV [17] which is, as expected, greater than those of Ni_3S_2 and NiS. There are no XPS binding energies available for the other binary nickel sulphides.

The surface properties of nickel sulphides are not of direct importance to the flotation separation of nickel-bearing ores, since nickel appears in economic sulphide ores in multi-metal phases of which the most important is pentlandite, $(Fe, Ni, Co)_9S_8$. However, the binary nickel sulphides provide model systems for the development of an understanding of the reactions of nickel in sulphide systems that is valuable in interpreting the behaviour of the more complex multi-component phases. In the work reported here. The complementary techniques of voltammetry and electron spectroscopy have been applied to elucidate the surface oxidation of heazlewoodite.

2. Experimental details

2.1. *Heazlewoodite*

A sintered compact of nickel powder was treated in a 4 : 1 H_2/H_2S atmosphere at 380° C to produce a dense, coherent sulphide layer 2 mm thick on the surface. XRD analysis confirmed that this layer had the heazlewoodite structure.

2.2. *X-ray photoelectron spectroscopy*

For XPS studies, fresh surfaces were created by abrading the surface on P 1000 silicon carbide paper in a nitrogen-flushed glove box attached to the entry port of the spectrometer. A natural sample of millerite (NiS) was also investigated and fresh surfaces were established in the same manner as for the other nickel sulphide.

The specimens were cooled to 150 K before the pressure was taken below 10^{-3} Pa and they were maintained at this temperature during exposure to the non-monochromatized X-rays (Mg source operated at 10 kV, 10 mA) at 10^{-7} Pa. This procedure was followed to avoid the possibility of volatilization of any elemental sulphur that may have been formed on the sulphide surface. Electron spectra were obtained with a Vacuum Generators ESCA 3 spectrometer at an analyser pass energy of 20 eV and slit width of 2 mm. Under these conditions, the $4f_{7/2}$ photoelectron peak from gold metal had a width of 1.05 eV and a binding energy of 83.8 eV. Spectra are shown normalized by the difference between the maximum and minimum number of counts. The binding energy of the $2p_{3/2}$ component is used to represent the position of a S(2p) doublet.

2.3. *Voltammetry*

A heazlewoodite electrode was prepared by cutting a 7 mm × 8 mm block from the sulphidized compact, attaching the block to a brass rod with conducting epoxy cement (ACME E-Solder) and encapsulating in epoxy resin (Araldite D). The brass rod was tapped to fit the threaded rotating spindle of a Beckmann variable speed rotating electrode system. The epoxy was cut back to expose the sulphide surface. A fresh surface was generated by abrasion on grade P 1000 silicon carbide paper in a nitrogen atmosphere and the electrode was immediately transferred to the electrochemical cell without exposure to air.

Voltammetry was also carried out with a carbon paste electrode. In these experiments, the heazlewoodite was stripped from the nickel compact, crushed and ground to a fine powder. The powder was then incorporated into the surface of the carbon paste electrode.

Voltammetric investigations were carried out at 21° C in solutions of pH 4.6 (0.5 M) acetic acid; 0.5 M sodium acetate), pH 9.2 (0.05 M sodium tetraborate); pH 13 (0.1 M potassium hydroxide). Studies were also conducted in the pH 4.6 solution containing 10^{-2} M nickel sulphate.

A PAR 173 potentiostat programmed with a Utah model 0151A sweep generator was used to control the potential and currents were recorded on a Yew type 3086 X-Y recorder. Potentials were measured against a saturated calomel electrode (SCE) and converted to the standard hydrogen electrode (SHE) scale assuming the SCE has a potential of 0.245 V with respect to the SHE [18].

3. Results and discussion

3.1. *X-ray photoelectron spectroscopy*

The Ni(2p) and S(2p) spectra from freshly abraded Ni_3S_2 are shown in Figs 1a and 2a, respectively. The $Ni(2p)_{3/2}$ peak near 855.7 eV, and the associated excited final state satellite near 861.5 eV, indicated the presence of one or more nickel-oxygen species at the sulphide surface, most probably hydrated nickel oxide.

The S(2p) spectrum in Fig. 2a consists of a major doublet at 162.2 eV, with components asymmetrically broadened on the high binding energy side. This doublet is assigned to Ni_3S_2. Each nickel atom in heazlewoodite occupies a pseudotetrahedral site in an approximately body-centred cubic sulphur lattice, and as well as being co-ordinated to these 4 sulphur atoms, there are 4 nickel atoms at ~0.25 nm [1]. Such very short metal–metal distances are indicative of intermetallic bonds; indeed, heazlewoodite has metallic electrical properties [1]. Consequently, a photoelectron peak is expected to display asymmetry as a result of the screening response of the conduction electrons to the sudden creation of the core hole [19–21]. The binding energy found for Ni_3S_2 is in agreement with that reported by Marcus *et al.* [7].

The S(2p) spectrum in Fig. 2a also includes a minor doublet at 161.4 eV, the 3/2 component of which is just evident as a shoulder on the low binding energy edge of the major $2p_{3/2}$ peak. A freshly abraded surface of millerite gave rise to a S(2p) spectrum at 161.4 eV which is similar to that reported by Grzetic [16]. Hence, the additional doublet on the spectrum from heazlewoodite is consistent with the presence of

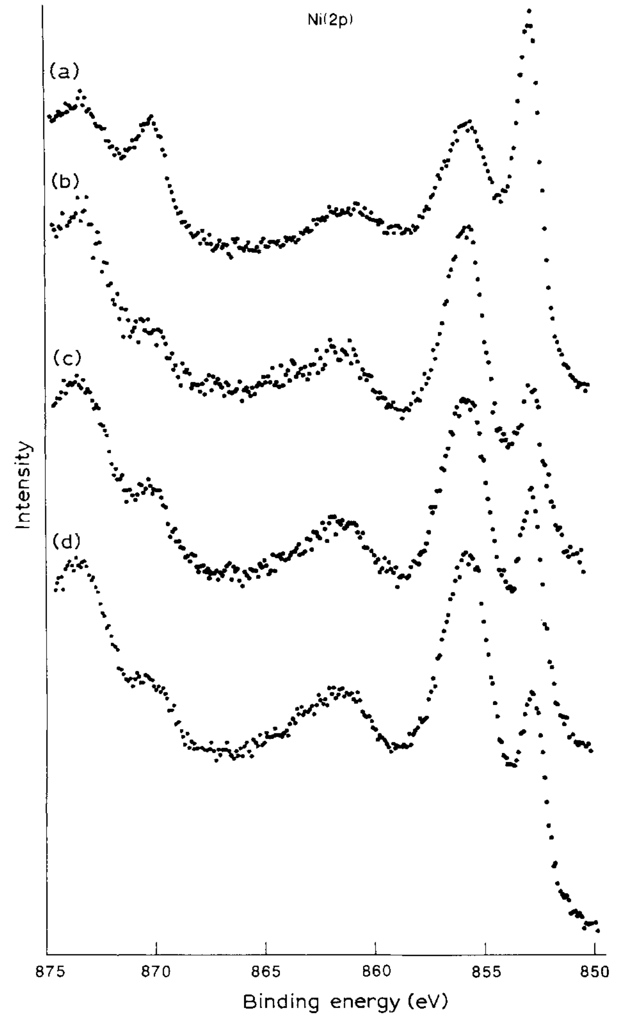

Fig. 1. Ni(2p) spectra from Ni_3S_2: (a) freshly abraded surface; (b) after exposure to the atmosphere for 16 h; (c) and (d) after immersion in acetic acid solution in equilibrium with air for 5 min (c) and 1 h (d).

a low concentration of NiS. No phases other than heazlewoodite were detected in the Ni_3S_2 sample by XRD analysis so the NiS, and associated nickel oxide, would appear to have arisen from surface oxidation despite the approach adopted to minimize contact with oxygen. However, it should be noted that the XRD technique would not detect phases present at levels below ~5%. The oxidation reaction can be represented by

$$Ni_3S_2 + \tfrac{1}{2}O_2 + H_2O \longrightarrow 2NiS + NiO \cdot H_2O \quad (1)$$

The Ni(2p) spectrum from heazlewoodite that had been exposed to the atmosphere for 16 h following the generation of a fresh surface by abrasion is shown in Fig. 1b. Clearly, the primary and satellite $2p_{3/2}$ peaks arising from hydrated nickel oxide were significantly greater than those for nickel in the sulphide lattice. The O(1s) spectrum, which was also more intense than for a freshly abraded surface, was consistent with a hydrated oxide since the peak was at 531.5 eV and there was no evidence for a shoulder near 530 eV that would have indicated the presence of unhydrated NiO. Despite the oxidation of the sulphide to form hydrated nickel oxide, the corresponding S(2p) spectrum (Fig. 2b) was essentially the same as that for a

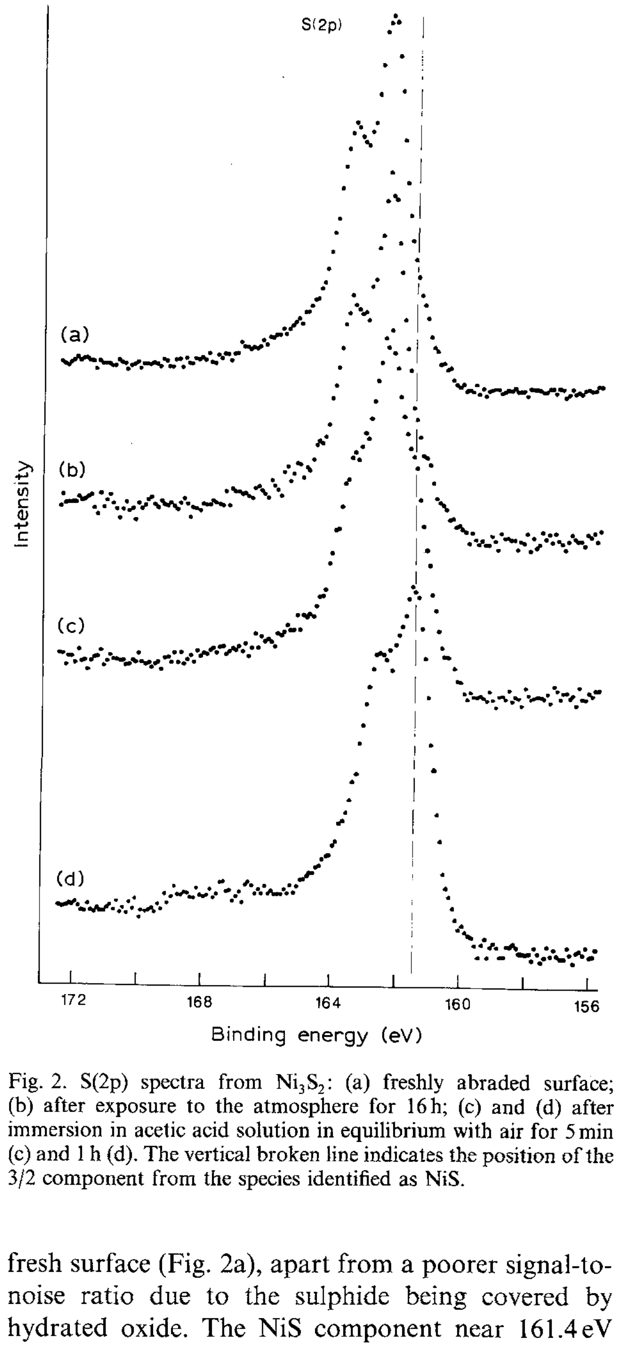

Fig. 2. S(2p) spectra from Ni_3S_2: (a) freshly abraded surface; (b) after exposure to the atmosphere for 16 h; (c) and (d) after immersion in acetic acid solution in equilibrium with air for 5 min (c) and 1 h (d). The vertical broken line indicates the position of the 3/2 component from the species identified as NiS.

fresh surface (Fig. 2a), apart from a poorer signal-to-noise ratio due to the sulphide being covered by hydrated oxide. The NiS component near 161.4 eV was not enhanced, and no components appeared at binding energies above 162.2 eV that would indicate the formation of sulphur–oxygen species. Thus, the sulphur atoms retain the heazlewoodite environment as nickel atoms are removed due to migration to the surface and combination with oxygen. The high temperature polymorph, high heazlewoodite (> 556° C) exhibits a wide range of non-stoichiometry [1] and it is possible that metastable, sulphur-rich heazlewoodite is formed in the surface region at ambient temperatures,

$$Ni_3S_2 + \tfrac{1}{2}xO_2 + xH_2O \longrightarrow Ni_{3-x}S_2 + xNiO \cdot H_2O \quad (2)$$

Note that the binding energies for Ni_7S_6 are not known and hence the formation of this phase is not ruled out by the XPS data.

It is difficult to explain why NiS was observed on a heazlewoodite surface that had had minimum contact with oxygen but is not the product of oxidation on extended exposure to air. It is possible that NiS was originally present in the heazlewoodite specimen but could not be detected by XRD analysis. Alternatively, the NiS could be the initial product and that further transfer of nickel to the surface leaves an underlying zone of nonstoichiometric heazlewoodite.

Study of the behaviour in dilute acetic acid has proved useful in identifying the products of the surface oxidation of sulphide minerals [8–13]. The acidity of such a solution is too low to cause non-oxidative dissolution, but is sufficient for the metal component to be soluble under oxidizing conditions. Thus, it has been possible to examine the sulphur oxidation products in the absence of overlying metal oxides.

The Ni(2p) and S(2p) spectra from Ni_3S_2 abraded under dilute acetic acid and immersed in 0.2 M acetic acid for 5 min are shown in Figs 1c and 2c, respectively. Corresponding spectra after immersion for 1 h are presented in Figs. 1d and 2d. In Fig. 2c, the major S(2p) doublet remains at 162.2 eV, but the (1/2, 3/2) components are less well resolved, and the shoulder on the low binding energy edge is more obvious due to a more intense minor doublet at ~ 161.4 eV. The latter binding energy corresponds to that of NiS. In Fig. 2d, the major S(2p) doublet is now at 161.4 eV and there is only a minor contribution at 162.2 eV from residual nickel-rich sulphide. There is also a broad contribution in the 166–169 eV region which indicates a small amount of sulphur-oxygen species as present.

In Figs. 1c and 1d, the Ni(2p) peaks from hydrated nickel oxide are appreciably more intense than those from nickel sulphide. The formation of nickel oxide on the sulphide surface as a result of treatment in acetic acid is surprising since sulphur is incorporated in nickel electroplating anodes to inhibit passivation [22, 23], and nickel plating baths operate at pH values of around 4. The mode of operation of such sulphur-depolarized anodes is considered [7] to involve the development of a surface layer of Ni_3S_2 that impedes the formation of nickel oxide. The hydrated oxide formed in acetic acid media may not be passivating since oxidation of Ni_3S_2 is not halted. After immersion in the acetic acid solution for 40 h, no sulphur or nickel peaks from nickel sulphide were detected due to a thick overlayer of hydrated nickel oxide. A small S(2p) peak was observed but this corresponded to that expected for sulphate. On the other hand, the presence of a solid oxide phase would be expected to retard nickel dissolution to a significant degree. This apparent contradiction could be explained by the formation of nickel oxide occurring in the acetic acid medium only when the outermost sulphide layer is the oxidation product, NiS, rather than a sulphide of higher nickel content.

Little information on the further oxidation of the NiS surface layer was obtained from the investigation with the acetic acid solution because of the development of the oxide layer. The observation of a small amount of sulphate, however, suggests that this species is produced rather than NiS_2 or elemental sulphur.

3.2. *Voltammetry*

Voltammograms for an Ni_3S_2 surface in pH 4.6 solution with stationary and rotated electrodes are shown in Figs. 3a and 3b, respectively. The only discernible difference between the two sets of curves is in the low potential region. It can be seen that, for both stationary and rotated electrodes, the current on the initial positive-going scan increased from the open-circuit potential of −0.25 V. This current arises from removal of nickel to form a sulphide of lower nickel content. The XPS results suggest that the initial reaction is

$$Ni_3S_2 \longrightarrow Ni_{3-x}S_2 + xNi^{2+} + 2xe^- \qquad (3)$$

and that, subsequently, NiS is formed:

$$Ni_3S_2 \longrightarrow 2NiS + Ni^{2+} + 2e^- \qquad (4)$$

The standard potential of Reaction 4, calculated from the Gibbs free energy of formation data tabulated by Vaughan and Craig [1], is 0.11 V. Thus, NiS can be formed in the potential region of the increasing anodic current in Fig. 3.

Evidence for the formation of a sulphur-rich heazlewoodite was obtained from rest potential measurements in a deoxygenated 10^{-2} M Ni^{2+} solution of pH 4.6. The potential of a surface after abrasion in nitrogen reached a constant value after 30 min of −0.214 V. The potential of a surface that had been immersed for 1 h in a pH 4.6 solution in equilibrium with air, under which conditions the XPS investigations show NiS to be formed, gave a constant rest potential after 30 min in the deoxygenated nickel solution of −0.13 V. The different rest potentials indicate different potential-determining couples. The potential for the freshly ground surface would correspond to an $Ni_{3-x}S_2$/NiS coupled with x being the after exposure to air-saturated solution would correspond to an $Ni_{3-x}S_2$/NiS coupld with x being the upper limit of metastability of heazlewoodite.

When the upper potential limit of the scan in Fig. 3 was below 0.3 V, a cathodic current wave was observed on the return scan for the stationary electrode due to the reverse of Reaction 3 or 4. This wave was absent for the rotated electrode because Ni^{2+}, produced by Reaction 3 and 4, was dispersed. In this case, sulphur in the nickel sulphide product is reduced according to

$$Ni_{3-x}S_2 + (4x/3)H^+ + (4x/3)e^- \longrightarrow \{(3-x)/3\}Ni_3S_2 + (2x/3)H_2S \qquad (5)$$

or,

$$3NiS + 2H^+ + 2e^- \longrightarrow Ni_3S_2 + H_2S \qquad (6)$$

Since some Ni^{2+} ions diffuse away from a stationary electrode, a current due to Reaction 5 or 6 was also observed in Fig. 3a. The NiS can oxidize further to elemental sulphur,

$$NiS \longrightarrow Ni^{2+} + S + 2e^- \qquad (7)$$

The anodic current increased to a maximum at

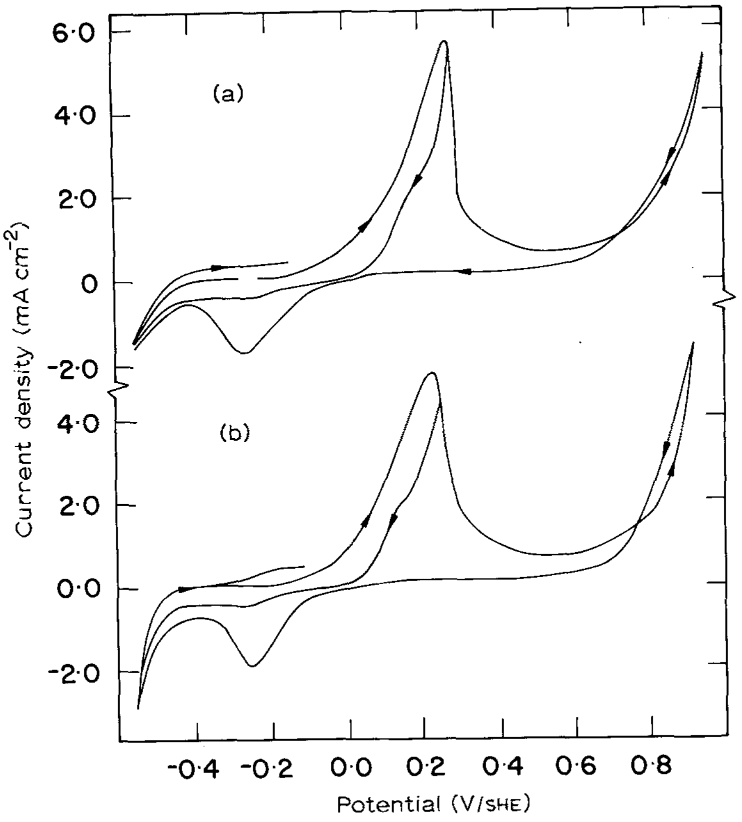

Fig. 3. Voltammograms for Ni_3S_2 electrode in pH 4.6 solution. A fresh surface formed in a nitrogen atmosphere before each scan. Sweeps at $20\,mV\,s^{-1}$ taken initially in the positive-going direction and reversed at different upper potential limits. Electrode (a) stationary and (b) rotated at 10 Hz.

about 0.25 V and then the oxidation became inhibited by one of the products of oxidation (Fig. 3). The charge passed before passivation occurred was $65\,mC\,cm^{-2}$, which corresponds to removal of nickel from a significant surface region.

When the potential was taken above 0.6 V, the anodic current increased again. Also, a cathodic peak appeared on the subsequent return scan at potentials expected for reduction of elemental sulphur,

$$S + 2H^+ + 2e^- \longrightarrow H_2S \qquad E^0 = 0.14\,V \quad (8)$$

If only nickel sulphides and sulphur are formed, and the nickel ions produced are dispersed, the ratio of the anodic and cathodic charges would be 1.5, since the number of electrons per sulphur atom in Reactions 4 and 7 is 3 while that in Reaction 8 is 2. Sulphate can be formed in addition to sulphur and this species will not be reduced on a subsequent negative-going scan. Thus, the balance between anodic and cathodic charges on the voltammogram provides a measure of the ratio of sulphur to sulphate formed in the oxidation process. This procedure was employed to determine the ratio of sulphur to sulphate produced in the surface oxidation of pyrite and pyrrhotite [24].

Since the anodic charges for Ni_3S_2 were much greater than the cathodic charges, particularly for the higher upper potential limit in Fig. 3, it is apparent that some sulphate was formed

$$Ni_3S_2 + 8H_2O \longrightarrow 3Ni^{2+} + 2SO_4^{2-} + 16H^+ + 18e^- \quad (9)$$

In basic solutions (Fig. 4), the anodic currents were much smaller than those observed at pH 4.6. This can be explained by nickel oxide now being the nickel product. That is, the initial oxidation of heazlewoodite will be

$$Ni_3S_2 + 2xH_2O \longrightarrow Ni_{3-x}S_2 + xNi(OH)_2 + 2xH^+ + 2xe^- \quad (10)$$

The inhibiting effect of nickel oxide would indicate that the appearance of this species in acetic acid solutions, identified by XPS (*v.s.*), occurs only in the passivation region.

As at pH 4.6, further oxidation can occur to NiS and elemental sulphur. However, the nickel oxide formed on the surface at pH 9.2 inhibits further oxidation and hence the anodic charges passed on the voltammogram in basic solutions were an order of magnitude less than those at pH 4.6. The increase in anodic current at ~0.7 V in Fig. 4b is due to the oxidation of nickel (II) oxide to nickel (III) oxide. The reverse process gives rise to the cathodic peak at the beginning of the return scan. The nickel (II)/ nickel (III) oxide features are not present in Fig. 4a because the potential of this redox couple is above the upper potential limit of the scan at pH 9.2.

Since nickel is retained at the electrode surface as a hydrated nickel oxide in basic solutions, the cathodic reactions on the return scans in Fig. 4 will correspond to the reverse of the anodic processes, provided the sulphur content is not oxidized beyond the elemental state. Thus, under these conditions, the anodic and cathodic charges should balance. An excess anodic charge would then indicate sulphate formation. However, the voltammograms for heazlewoodite do not allow an accurate balance between anodic and cathodic charges to be obtained in basic media because

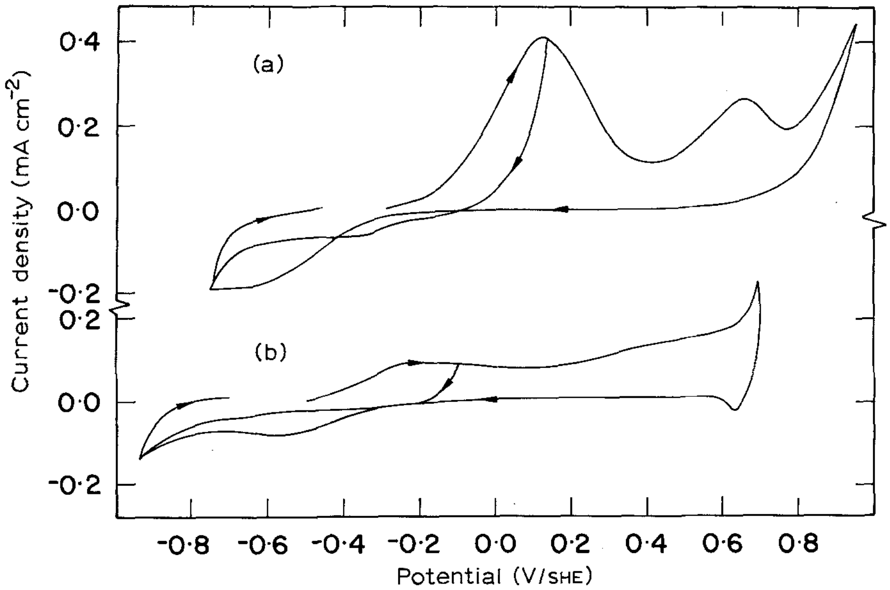

Fig. 4. Voltammograms for Ni_3S_2 electrode in solutions of (a) pH 9.2 and (b) pH 13. A fresh surface formed in a nitrogen atmosphere before each scan. Sweeps at $20\,mV\,s^{-1}$ taken initially in the positive-going direction and reversed at different upper potential limits.

reduction of the products of oxidation is not complete before Ni_3S_2 is itself reduced. However, the relative charges passed indicate that, for short scans, sulphur species are the major product, whereas it is sulphate on the scans to the higher upper potential limits.

Price and Davenport [6] concluded that the oxidation of Ni_3S_2 in acid media proceeded through a series of individual nickel sulphide phases of progressively lower nickel content. The potentials realized in their work were above 1 V, which is higher than the values explored in Fig. 3. To determine whether such sulphides are formed at lower potentials, investigations of the anodic oxidation of Ni_3S_2 particles were undertaken at very slow scan rates using a carbon paste electrode. In studies of the anodic oxidation of Cu_2S to CuS [25, 26], this approach allowed intermediate copper sulphides to be differentiated because the complete particles were converted to each intermediate phase before oxidation to the subsequent phase commenced. To compare the potentials at which the product phases are formed with reversible values calculated from Gibbs free energy values, it is necessary to include a known concentration of the dissolving ion in the solution. The studies with Ni_3S_2 were carried out in pH 4.6 solution containing 10^{-2} Ni^{2+}. Before voltammograms were recorded, oxidation products formed in the grinding of the sulphide were reduced back to Ni_3S_2 by holding the potential at -0.25 V until the cathodic current decreased to a negligible value. Ni_3S_2 can be regenerated by the reverse of Reaction 10 and, with nickel in solution, by the reverse of Reactions 3 and 4. Voltammograms recorded at $0.18\,mV\,s^{-1}$ following the pretreatment are presented in Fig. 5. The anodic current rises to a peak at 0.0 V and then decreases to a low value at 0.2 V. Note that pretreatment at potentials more negative than -0.25 V resulted in the deposition of nickel metal and this gave rise to an additional anodic peak at potentials below that for Ni_3S_2 oxidation.

The potential region covered by the anodic peak in Fig. 5 extends over the complete stability region from Ni_3S_2 to NiS_2. The reversible potentials in 10^{-2} M Ni^{2+}, calculated from the Gibbs free energy of formation data reported by Vaughan and Craig [1], are: Ni_3S_2/Ni_7S_6, -0.127 V; Ni_7S_6/NiS, -0.170 V; NiS/Ni_3S_4, -0.029 V; and Ni_3S_4/NiS_2, 0.001 V. Note that the first two values indicate that Ni_7S_6 is not a stable phase, but this probably arises from a slightly inaccurate value of the Gibbs free energy reported for this sulphide. In order to determine whether the anodic peak corresponds to complete oxidation to NiS_2, or to one of the intermediate phases, an experiment was carried out in which the potential was swept to 0.1 V

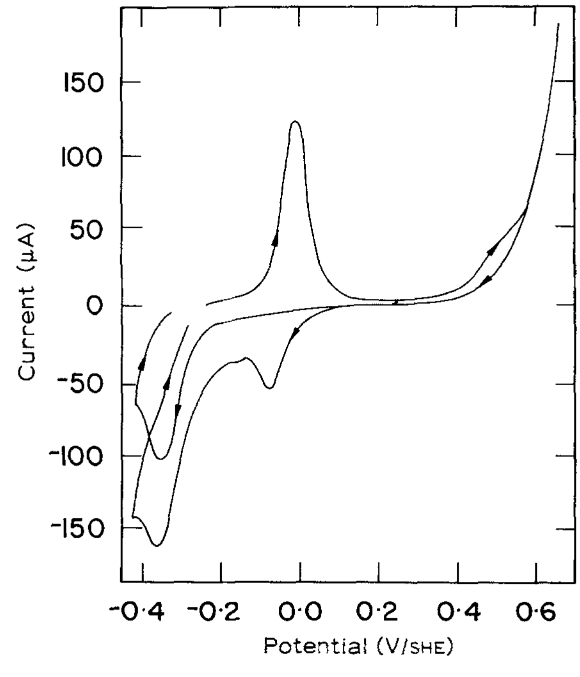

Fig. 5. Voltammograms for ground Ni_3S_2 in carbon paste electrode in 10^{-2} M Ni^{2+} solution of pH 4.6. Electrode held at -0.25 V and then scans run at $0.18\,mV\,s^{-1}$ in the positive-going direction and reversed at different upper potential limits.

and held at this value for 63 h. The outer layer of the carbon paste electrode, including the nickel sulphide, was then removed. XRD analysis of this material revealed only the patterns characteristic of heazlewoodite and carbon. The heazlewoodite peaks were broadened, and this could be explained by the loss of some nickel without changing the lattice structure. Thus, it would appear that the anodic peak arises largely from removal of nickel to form a sulphur-rich heazlewoodite.

The S(2p) photoelectron spectrum from an Ni_3S_2 surface after treatment in acetic acid solution in equilibrium with air was consistent with the presence of NiS plus a sulphur-rich heazlewoodite (*v.s.*). The open circuit potential of an Ni_3S_2 electrode in 10^{-2} Ni^{2+} solution of pH 4.6 in equilibrium with air was found to be -0.02 V, which is close to the peak potential in Fig. 5. Thus, the XPS investigations would indicate that the anodic peak corresponded to oxidation only as far as NiS and that this species was restricted to a surface layer. Presumably the surface becomes passivated by the NiS and/or by the hydrated nickel oxide layer that the XPS investigations revealed was associated with NiS formation.

The above interpretation of the anodic peak implies that further oxidation of NiS requires significant overpotentials and is associated with the anodic wave that commences at 0.3 V (Fig. 5). This conclusion is in agreement with investigations of the anodic behaviour of millerite electrodes in solutions of pH 0 [4] that showed no oxidation current below ~0.7 V.

When nickel ions are present in solution, the reactions giving rise to the cathodic charge on the voltammogram will be the reverse of Reactions 3, 4 and 7. Thus, under these experimental conditions, the anodic and cathodic charges should balance, provided sulphur is not oxidized beyond the elemental state. The ratio of cathodic to anodic charges on the voltammogram in Fig. 5 is close to unity for the scan to 0.2 V, but is above 2 for that to 0.67 V. This indicates that some sulphate was formed in the high potential region.

The return scan from 0.67 V in Fig. 5 displays major peaks at -0.08 V and -0.35 V with a minor peak at -0.15 V and a shoulder at -0.2 V. The peak at -0.35 V can be assigned confidently to the re-formation of Ni_3S_2 since this peak is evident on scans to lower upper-potential limits. The other characteristics arise from the reduction of oxidation products of NiS and the multiplicity of features indicates that a range of sulphides as well as elemental sulphur could be present. However, the potential region in which these higher sulphides are formed is much greater than that attained by exposure to solutions in equilibrium with air.

Voltammograms were also recorded at very slow scan rates with the bulk Ni_3S_2 electrode in 10^{-2} M nickel sulphate solution of pH 4.6 (Fig. 6). The anodic current increased to a peak at -0.03 V, similar to the behaviour of Ni_3S_2 with the carbon paste electrode, but a second peak appeared at 0.13 V and a shoulder between 0.2 and 0.45 V. On the return scan from a sweep to 0.68 V, anodic current was observed in the upper potential region and this actually increased between 0.25 and 0.1 V. The most likely explanation of these additional features is that changes to the surface NiS layer allow access to the underlying heazlewoodite and removal of nickel from a greater depth becomes possible.

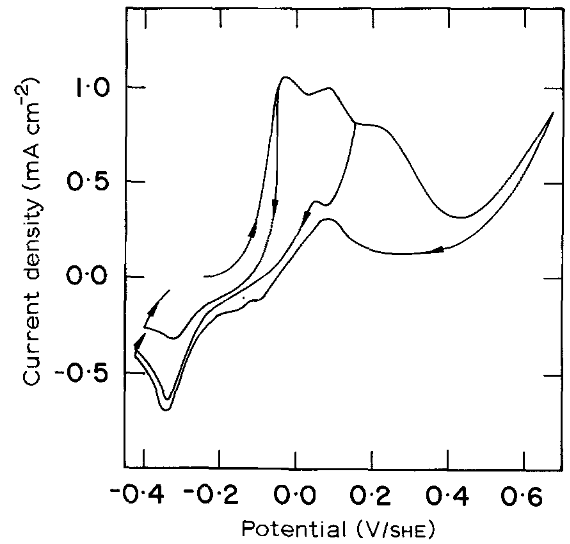

Fig. 6. Voltammograms for Ni_3S_2 electrode in 10^{-2} M Ni^{2+} solution of pH 4.6. A fresh surface formed in a nitrogen atmosphere before each scan. Sweeps at 0.18 mV s^{-1} taken initially in the positive-going direction and reversed at different upper potential limits.

It can be seen that multiple cathodic peaks are evident in Fig. 6 on the return scan from 0.68 V and this supports the hypothesis that a number of different nickel sulphide products were formed in the high potential region.

4. Conclusion

The results of both voltammetric and electron spectroscopic investigations show that heazlewoodite oxidizes readily to form a sulphur-rich heazlewoodite phase. In addition, there is evidence for some reconstruction to form a surface layer of NiS. The nickel sulphides differ from other metal sulphides in that the sulphur binding energies of the metal-rich phase are greater than those of the monosulphide. Thus, a higher S(2p) binding energy cannot be taken as an indicator of an increase in metal deficiency at nickel-containing sulphide surfaces, as has been established to be the case for other sulphide minerals.

Acknowledgements

The authors are indebted to R. C. A. Flann for preparation of the heazlewoodite and to K. J. McDonald for XRD analysis.

References

[1] D. J. Vaughan and J. R. Craig, 'Mineral chemistry of metal sulfides', Cambridge University Press, Cambridge (1978).

[2] T. Kato and T. Oki, *Japan Inst. Met. J.* **37** (1973) 1338.

[3] *Idem*, *Nippon Kinoku Gakkaishi* **38** (1974) 663.

[4] G. P. Power, *Aust. J. Chem.* **34** (1981) 2287.

[5] *Idem*, *Electrochim. Acta* **27** (1982) 359.

[6] D. C. Price and W. G. Davenport, *J. Appl. Electrochem.* **12** (1982) 281.

[7] P. Marcus, J. Oudar and I. Olefjord, *Mater. Sci. Eng.* **42** (1980) 191.

[8] A. N. Buckley and R. Woods, *Aust. J. Chem.* **36** (1983) 1793.

[9] *Idem*, *Appl. Surf. Sci.* **17** (1984) 401.

[10] *Idem*, *ibid.* **22/23** (1985) 280.

[11] *Idem*, *ibid.* **20** (1985) 472.

[12] A. N. Buckley, R. Woods and H. J. Wouterlood, in 'Proc. Int. Symp. Electrochemistry in Mineral and Metal Processing II', (edited by P. E. Richardson and R. Woods), Electrochem. Soc., Pennington; NJ (1988) pp. 211–33.

[13] A. N. Buckley and R. Woods, *Appl. Surf. Sci.* **27** (1987) 437.

[14] P. J. Reucroft and R. B. Shalvoy, *Surf. Interface Anal.* **3** (1981) 86.

[15] P. Broutin, J. J. Ehrhardt, A. Pentenero and J. M. Gras, *J. Microsc. Spectrosc. Electron.* **9** (1984) 57.

[16] I. Grzetic, *J. Eng. Phys.* **26** (1984) 16.

[17] H. van der Heide, R. Hemmel, C. F. van Bruggen and C. Haas, *J. Solid State Chem.* **33** (1980) 17.

[18] R. G. Bates, 'Determination of pH', Wiley, New York, NY (1964) p. 278.

[19] S. Doniach and M. Sunjic, *J. Phys. C* **3** (1970) 285.

[20] G. K. Wertheim, F. J. DiSalvo and S. Chiang, *Phys. Rev. B* **13** (1976) 5476.

[21] G. K. Wertheim and D. N. E. Buchanan, *Phys. Rev. B* **16** (1977) 2613.

[22] 'The Canning Handbook on Electroplating', Canning, Birmingham (1978) p. 376.

[23] C. M. Whittington, 'Metals Australasia', 26 September and 21 October (1979).

[24] I. C. Hamilton and R. Woods, *J. Electroanal. Chem.* **118** (1981) 327.

[25] M. C. Bruge, M. Lamache and D. Bauer, *Electrochim. Acta* **24** (1979) 25.

[26] J. Gerlach and E. Kuzeci, *Hydromet.* **11** (1983) 345.